THE JOURNAL OF BIOLOGICAL CHEMISTRY
Vol. 278, No. 52, Issue of December 26, pp. 52826–52833, 2003
Printed in U.S.A.

Crystal Structure of Wild-type Penicillin-binding Protein 5 from *Escherichia coli*

IMPLICATIONS FOR DEACYLATION OF THE ACYL-ENZYME COMPLEX*

Received for publication, September 12, 2003, and in revised form, October 9, 2003
Published, JBC Papers in Press, October 10, 2003, DOI 10.1074/jbc.M310177200

Robert A. Nicholas‡§, Sandra Krings¶, Joshua Tomberg‡, George Nicola¶, and Christopher Davies¶‖

From the ‡Department of Pharmacology, University of North Carolina, Chapel Hill, North Carolina 27599-7365 and the ¶Department of Biochemistry & Molecular Biology, Medical University of South Carolina, Charleston, South Carolina 29425

Penicillin-binding protein 5 (PBP 5) of *Escherichia coli* functions as a D-alanine carboxypeptidase (CPase), cleaving D-alanine from the C terminus of cell wall peptides. Like all PBPs, PBP 5 forms a covalent acyl-enzyme complex with β-lactam antibiotics; however, PBP 5 is distinguished by its high rate of deacylation of the acyl-enzyme complex ($t_{½} \approx 10$ min). A Gly^{105} → Asp mutation in PBP 5 markedly impairs deacylation with only minor effects on acylation, and abolishes CPase activity. We have determined the three-dimensional structure of a soluble form of wild-type PBP 5 at 1.85-Å resolution and have also refined the structure of the G105D mutant form of PBP 5 to 1.9-Å resolution. Comparison of the two structures reveals that the major effect of the mutation is to disorder a loop comprising residues 74–90 that sits atop the SXN motif of the active site. Deletion of the 74–90 loop in wild-type PBP 5 markedly diminished the deacylation rate of penicillin G with a minimal impact on acylation, and abolished CPase activity. These effects were very similar to those observed in the G105D mutant, reinforcing the idea that this mutation causes disordering of the 74–90 loop. Mutation of two consecutive serines within this loop, which hydrogen bond to Ser^{110} and Asn^{112} in the SXN motif, had marked effects on CPase activity, but not β-lactam antibiotic binding or hydrolysis. These data suggest a direct role for the SXN motif in deacylation of the acyl-enzyme complex and imply that the functioning of this motif is modulated by the 74–90 loop.

Bacterial cell wall peptidoglycan surrounds the cell and is essential for proper maintenance of cellular morphology and cell viability. In *Escherichia coli*, cell walls are composed of a repeating disaccharide, *N*-acetylglucosamine-β-1,4-*N*-acetylmuramic acid, in which the muramic acid residues are substituted with the pentapeptide, L-Ala-D-γ-Glu-*m*-DAP-D-Ala-D-Ala (where m-DAP = *meso*-diaminopimelic acid). During peptidoglycan synthesis, disaccharide-pentapeptide units are polymerized onto nascent glycan chains (transglycosylation) and the peptide chains from different glycan strands are cross-linked (transpeptidation) by transpeptidases known as penicillin-binding proteins or PBPs.[1] Cross-linking of the peptide chains confers rigidity to the peptidoglycan and viability to the bacterial cell. The related carboxypeptidases, which hydrolyze the C-terminal D-Ala moiety from the peptide chain, may modulate the degree of cross-linking.

In *E. coli* at least 10 PBPs have been identified. These enzymes fall into two categories: the high molecular mass PBPs, which are essential for cell viability and catalyze transpeptidase and sometimes transglycosylase activity, and the low molecular mass PBPs, which are non-essential and catalyze D,D-carboxypeptidase (CPase) and sometimes D,D-endopeptidase activity (1). Regardless of the type of PBP, all of these enzymes react with peptide substrates and β-lactam antibiotics by a similar mechanism. The initial step in the reaction of PBPs with their peptide substrates is a nucleophilic attack of the D-Ala-D-Ala peptide bond by a conserved serine residue, leading to acylation of the serine hydroxyl side chain and the concomitant release of the C-terminal D-Ala. In the subsequent deacylation step, the acyl-enzyme complex can react with either an amino group (from *m*-DAP) of another peptide to form a cross-link (transpeptidation) or it can react with water to release the peptide (carboxypeptidation). Penicillin and other β-lactam antibiotics inactivate these enzymes by mimicking the structure of the D-Ala-D-Ala C terminus of the peptide chain (2, 3) and reacting with the same serine nucleophile to form an analogous acyl-enzyme complex (4). Unlike the complex formed with peptide substrates, however, the β-lactam-PBP complex is long-lived and renders the enzyme inactive.

PBPs and other penicillin-interacting enzymes (*e.g.* class A β-lactamases) are characterized by a set of conserved motifs that are clustered in their respective active sites (5). These motifs include the Ser-*X*-*X*-Lys (S*XX*K) tetrad that contains the serine nucleophile, the Ser-*X*-Asn (S*X*N) triad, and the Lys-Thr(Ser)-Gly (KTG) triad. In all serine-based PBPs and β-lactamases of known structure, these motifs adopt a strikingly similar conformation to the extent that the active site of one PBP or β-lactamase can look very much like another. In addition to these three motifs, class A β-lactamases have a fourth motif, Glu-*X*-*X*-*X*-Asn, present on the so-called Ω loop, that is responsible for the extremely high rates of deacylation of the

* This work was supported by National Institutes of Health Grants AI36901 (to R. A. N.) and GM66861 (to C. D.). The costs of publication of this article were defrayed in part by the payment of page charges. This article must therefore be hereby marked "*advertisement*" in accordance with 18 U.S.C. Section 1734 solely to indicate this fact.

§ To whom correspondence may be addressed: Dept. of Pharmacology, CB 7365 Mary Ellen Jones Bldg., Chapel Hill, NC 27599-7365. Tel.: 919-966-6547; Fax: 919-966-5640; E-mail: nicholas@med.unc.edu.

‖ To whom correspondence may be addressed: Dept. of Biochemistry and Molecular Biology, 173 Ashley Ave., Charleston, SC 29425-0001. Tel.: 843-792-1468; Fax: 843-792-8568; E-mail: davies@musc.edu.

[1] The abbreviations used are: PBP, penicillin-binding protein; CPase, carboxypeptidase; *m*-DAP, *meso*-diaminopimelic acid; LO, loop-out; r.m.s., root mean square.

antibiotic-β-lactamase complex (6–8). Despite a wealth of structural and biochemical data, a consensus on the definitive mechanism of catalysis in β-lactamases has yet to emerge. Nevertheless, the picture of catalysis by β-lactamases is much clearer than in the related PBPs.

To further our understanding of both acylation and deacylation in PBPs and to examine their mechanistic similarities with β-lactamases, we have focused on PBP 5 from *E. coli*. PBP 5 is one of the best characterized PBPs and provides an excellent system in which to study the catalytic mechanism of penicillin-interacting enzymes (9–11). PBP 5 is the most abundant PBP in *E. coli* and catalyzes the major D-alanine carboxypeptidase activity *in vivo* (12). Although it is not essential for cell viability, recent studies have shown that PBP 5 is required for proper cell morphology in *E. coli* missing certain PBPs (13) and that it may have a role in cell division (14). PBP 5 is unusual among PBPs in that it catalyzes a respectable β-lactamase activity ($t_{½} \approx 10$ min at pH 7.0) (15, 16). A deacylation-defective mutant of PBP 5 containing a Gly^{105} to Asp mutation (termed PBP 5′) was identified from a screen of bacterial strains lacking carboxypeptidase IA activity (17, 18). Kinetic studies demonstrated that PBP 5′ had near normal acylation rates with penicillin G, but displayed a 30-fold decrease in the rate of deacylation of the penicilloyl-PBP 5′ complex (16, 19). Recently, we reported the crystal structure of PBP 5′ (20), which revealed a conventional arrangement of active site motifs but, in the absence of the wild-type structure, provided few clues regarding the underlying reason for the defect in deacylation. In this paper we present the structure of wild-type PBP 5 solved to 1.85-Å resolution. This structure is compared with that of PBP 5′ now refined to the higher resolution of 1.9 Å. The principal difference in the wild-type structure is the ordering of a loop near the active site comprising residues 74–90, leading to the hypothesis that the disordering of this loop in the mutant enzyme is responsible for its markedly decreased deacylation rate. Kinetic data from mutants in which this loop was removed are consistent with this hypothesis. We also identify two conserved serine residues on this loop that are important for CPase activity.

MATERIALS AND METHODS

Crystallization—A soluble form of wild-type PBP 5 missing its cleavable signal sequence was expressed in the cytoplasm of *E. coli* BL21* cells (Invitrogen, Carlsbad, CA) and purified by ampicillin affinity chromatography as described previously (16). For crystallization experiments the protein was concentrated to 5.5 mg/ml in 20 mM Tris, pH 7.5, containing 30 mM NaCl and 3 mM β-mercaptoethanol. Wild-type PBP 5 did not crystallize under the same conditions as those used for PBP 5′ (20) and so a new search for conditions was undertaken. Initial trials used the vapor diffusion hanging drop technique in which 3 μl of protein was mixed with 3 μl of well solution. A wide variety of conditions were tested, including Crystal Screens I and II (Hampton Research, Laguna Niguel, CA). PBP 5′ was purified and crystallized according to previously established conditions (16, 20).

Data Collection—Crystals of both wild-type and G105D mutant PBP 5 were cryo-protected by passage through their respective stabilization solutions (wild-type PBP 5: 8% PEG 400, 50 mM Tris-HCl, pH 8.0; PBP 5′: 20% PEG 4000, 100 mM Tris, pH 7.0) containing increasing concentrations of glycerol, in 2% increments, up to a maximum of 25%. At each step the crystals were soaked for 5–10 min except at the final step where the crystals were soaked overnight. Data were collected on a RAXIS-IV++ imaging plate system mounted on an RU-H3R x-ray generator operating at 50 kV and 100 mA and fitted with Osmic Confocal Optics (Rigaku/MSC, The Woodlands, TX). For the wild-type crystals, the crystal-to-detector distance was set at 140 mm and data were collected in 0.5° oscillation frames with an exposure time of 5 min per frame. A total of 215° of data were collected. For PBP 5′ crystals, the crystal-to-detector distance was 150 mm and data were collected in 1°-oscillation frames with an exposure time of 5 min per frame. A total of 200° of data were obtained. Both data sets were processed with CrystalClear (21).

Structure Determination and Refinement—The starting model for both refinements was the previous 2.3-Å structure of PBP 5′ that had been refined against data obtained at room temperature (20). The structure of wild-type PBP 5 was solved by molecular replacement using AMoRe (22) with a search model of PBP 5′ in which Asp^{105} had been replaced by glycine. Initially, both models were refined with XPLOR (23), and included several rounds of rigid body refinement, but later rounds used REFMAC5 (24). Manual refitting of the structures was performed as necessary with O (25). Water molecules were included as they became visible in both the ($F_o - F_c$) and 2($F_o - F_c$) electron density maps and if they had at least two potential hydrogen bonding partners. The quality of the models was assessed by PROCHECK (26) and superimpositions were performed using LSQKAB (27). The coordinates and structure factors for the wild-type PBP 5 (1NZO) and PBP 5′ (1NJ4) structures have been deposited with the Protein Data Bank.

Construction and Purification of PBP 5 Variants—Constructs of PBP 5 were made in which residues 72–92 were deleted, termed "loop out" (LO). These constructs were made in both wild-type PBP 5 (PBP 5-LO) and in the G105D mutant (PBP 5′-LO). PBP 5-LO was constructed by 4-primer PCR as described previously (28). The outside primers were complementary to sequences surrounding the multiple cloning site in the pT7-7K vector (29). The LO-down internal primer was complementary to codons 64–71 and 93–98, inclusive (5′-CGGAACCTGCATGCCCGGGATAGTGACTAAATCAGTTTCTT-3′), whereas the LO-up internal primer (5′-CCGGGCATGCAGGTTCCG-3′) was complementary to codons 93–98. In the first round of PCR, pT7-PBP 5 was amplified with pT7-up and LO-down and with pT7-down and LO-up. Following the first round of PCR, the two fragments were isolated and added to a new tube with the outside primers only, and PCR was carried out as before. The overlapping regions allowed for the annealing of the two fragments and the full-length gene missing codons 72–92 of the mature PBP 5 sequence was generated. The final PCR product was digested with XbaI and HindIII and ligated into similarly digested pT7-7K to produce pT7-PBP 5-LO. To construct pT7-PBP 5′-LO, the XhoI-SphI fragment encompassing the 5′ end of the gene up to codon 94 of pT7 PBP 5-LO was ligated with the SphI-BglII fragment from pT7-PBP 5′ containing the G105D mutation and the BglII-XhoI vector fragment from pT7-7K. Individual mutations were constructed in a similar manner and cloned into the same vector as for the loop-out constructs. All constructs were verified by sequencing. Following transformation of the vectors into BL21* cells, the mutant proteins were purified by ampicillin affinity chromatography as described for PBP 5 and PBP 5′ (16).

Kinetic Analysis of the Interaction of PBP 5 Variants with [^{14}C]Penicillin G and Peptide Substrate—The reaction mechanism for the interaction of PBPs with peptide and β-lactam antibiotics is,

$$E + S \underset{k_{-1}}{\overset{k_1}{\longleftrightarrow}} E \cdot S \xrightarrow{k_2} E - S \xrightarrow{k_3} E + P \qquad \text{(Eq. 1)}$$

where, $K' = (k_{-1} + k_2)/k_1$, E·S is the non-covalent Michaelis complex, E-S is the covalent acyl-enzyme complex, and P is the released product. The constant k_2/K', which describes the formation of the acyl-enzyme complex (E-S) at low (subsaturating) concentrations of β-lactam antibiotics, was determined from time courses of the formation of E-S with [^{14}C]penicillin G essentially as described (30). PBP 5 (48 μg; 1.2 nmol) was diluted into 150 μl of binding buffer (50 mM sodium phosphate, pH 7.0, 10% glycerol) and mixed with an equal volume of 100 μM [^{14}C]penicillin G in binding buffer. At timed intervals, 20-μl aliquots were removed, mixed with 5 ml of 5% trichloroacetic acid (w/v), and incubated on ice for 15 min. The acidified proteins were passed through number 30 glass fiber filters (Schleicher and Schuell, Keene, NH) and the filters were washed twice with 5 ml each of 1% trichloroacetic acid, 33% methanol. The filters were then air dried, placed in scintillation vials with 3 ml of Scinti-safe scintillation fluid (Fisher Scientific, Pittsburg, PA), and counted.

k_3 values were determined from semi-log plots of the % [^{14}C]penicillin G remaining *versus* time. PBP 5 proteins (11–37 μg; 0.28–0.92 nmol) were diluted into 150 μl of binding buffer and mixed with an equal volume of 100 μM [^{14}C]penicillin G for 10 min at 30 °C. At $t = 0$, penicillin G was added to 3 mM, and the amount of radioactivity remaining covalently bound to the protein was determined by removing 20-μl aliquots at various times and quantitating the amount of bound [^{14}C]penicillin G as described above. The $t_{½}$ values were determined from the plots and converted to k_3 values by dividing the $t_{½}$ in seconds into 0.693.

CPase assays were carried out with the peptide N,N'-diacetyl-L-Lys-D-Ala-D-Ala and the amount of hydrolysis of the ultimate D-alanine

residue was quantitated with the spectrophotometric microtiter plate protocol described by Gutheil *et al.* (10). Assays contained from 0 to 10 mM peptide and 0.83 μM enzyme, with the exception that PBP 5′, PBP 5-LO, and PBP 5′-LO were also tested at 8.3 μM.

RESULTS

Structure Determination—Crystals of wild-type PBP 5 were obtained over wells containing 8% PEG 400, 100 mM Tris, pH 8.0. This condition is considerably different from that for PBP 5′ (20% PEG 4000, 50 mM Tris, pH 7.0 (16)) and indicates some difference in the protein structure. Diffraction studies revealed that the crystals belonged to space group C2 with cell dimensions a = 109.4 Å, b = 50.3 Å, c = 84.5 Å, and β = 120.9°. Electron density maps showed that the region between residues 74 and 90, which is absent in the structure of PBP 5′ because of apparent flexibility, is ordered in the wild-type structure. The R factor of the final model is 20.9% (R_{free} = 24.5%).

For the purposes of structure comparison a new data set under cryo conditions was obtained from crystals of PBP 5′. This resulted in a slight improvement in resolution (from 2.3 to 1.9 Å) compared with previous data collected at room temperature (20), but a significant improvement in completeness and redundancy. The cell dimensions under cryo conditions were $a = b$ = 50.2 Å and c = 136.8 Å, which differs principally from the room temperature cell through a 3.5-Å reduction in the c dimension. The structure was refined against the 1.9 Å data to a final R factor of 20.9% (R_{free} = 24.4%). Compared with the room temperature structure, residues 85–90 are now visible in the electron density map but residues 74–84 remain disordered. In both structures difficulty was encountered in fitting the region 154–157 because this appears to exhibit some disordering, thus weakening the electron density. The data collection and final refinement statistics of both models are shown in Table I.

TABLE I
X-ray diffraction data and model refinement statistics for wild-type and G105D mutant PBP 5 (PBP 5′) structures
Figures within brackets are for the outer resolution shells.

	Wild-type (1NZO)	PBP 5′ (1NJ4)
Data collection		
Resolution range (Å)	54.0-1.85 (1.92-1.85)	36.9-1.9 (1.97-1.90)
R_{merge}[a] (%)	6.0 (32.2)	7.3 (35.8)
Completeness (%)	93.4 (67.8)	98.7 (88.4)
$\langle I\rangle/\langle\sigma I\rangle$	7.4 (2.0)	7.1 (1.8)
No. of observations	141727	178730
No. of unique reflections	31624	29772
Redundancy	4.5	6.0
Refinement		
Resolution range (Å)	15.0-1.85	15-1.90
No. of reflections used in refinement	28942	28198
Reflections in Free R set (%)	5	5
No. of non-hydrogen protein atoms	2718	2649
No. of water molecules	190	219
R factor (%)	20.9	20.9
R work (%)	20.7	20.7
R free (%)	24.5	24.4
Overall B_{iso} (Å^3)	31.9	29.3
Mean B factor (main chain) (Å^3)	30.5	27.9
R.m.s. deviation in main chain B factor (Å^3)	0.56	0.51
Mean B factor (side chains) (Å^3)	32.7	29.8
R.m.s. deviation in side chain B factors (Å^3)	1.59	1.27
Mean B factor (waters alone) (Å^3)	37.5	34.9
R.m.s. deviation for bond length (Å)	0.013	0.007
R.m.s. deviation for angle distances (°)	1.51	1.21
Ramachandran plot		
Residues in most favored region (%)	91.5	92.6
Residues in disallowed regions (%)	0.0	0.0

[a] $R_{merge} = \Sigma|I_i - I_m|/\Sigma I_i$, where I_i is the intensity of the measured reflection and I_m is the mean intensity of all symmetry-related reflections.

Structure Description—The overall structure of wild-type PBP 5 exhibits the same fold as that previously described for PBP 5′ (20). Briefly, PBP 5 is composed of two domains that are oriented approximately at right angles to each other (Fig. 1*A*). Domain 1, which is a transpeptidase-like domain typical of penicillin-interacting enzymes, comprises a five-stranded anti-parallel β sheet packed on both sides by α helices. Domain 2 is unique to PBP 5 and is formed by a sandwich of two anti-parallel β sheets, one three-stranded and the other two-stranded. The active site of PBP 5 is located at the interface of the five-stranded anti-parallel β sheet and the large α helical cluster within domain 1.

Structure Comparison—The common main chain atoms of domain 1 of wild-type PBP 5 and PBP 5′ superimpose very closely with an r.m.s. deviation of 0.88 Å, indicating that the mutation has little effect on the overall structure. After superimposition a slight shift in the relative position of domain 2 is observed (Fig. 1*A*). This difference arises from a hinging motion centered at the domain boundary (residue 262) resulting in a relative 6-Å shift of residues at the base of domain 2. The shifted position of domain 2 is likely the result of crystal packing interactions, which are different in the two structures. In the wild-type structure the tip of domain 2 packs against the 74–90 loop, whereas in PBP 5′ this region is largely exposed.

Superimposition reveals two regions within domain 1 in which significant structural differences are observed between the wild-type and mutant enzymes: 1) residues 74–90, and 2) residues 190–193 of the β7-β8 loop (Fig. 1*B*). Slight differences are also seen in the so-called Ω-like loop, but because the electron density for this region is weak in both structures, this is most likely because of the difficulties in fitting the model.

74–90 Region—In the structure of PBP 5′ reported previously, which was solved using data collected at room temperature, the region between residues 74 and 90 (inclusive) was not visible in the electron density map (20). In the new structure of PBP 5′ refined against data collected under cryo conditions, residues 85–90 are now visible and adopt an irregular loop structure, whereas residues 74 to 84 remain disordered (Fig. 1*B*). The crystallographic B factors for residues 85–90, however, are high (in the 50s) and some of the side chains are poorly resolved, indicating a high degree of flexibility. The increased ordering of residues 85–90 in PBP 5′ is likely because of the improvement in the quality of data obtained under cryogenic conditions. In contrast, the entire region encompassing 74–90 in the wild-type structure is highly ordered and has refined with low B factors (in the 30s). The secondary structure of this region, which is stabilized by numerous non-bonding interactions to the surrounding protein, is mostly an irregular loop but starts with a helical turn and finishes in an extended conformation. In the middle is a striking "zig zag" motif in which there are tight turns made by Pro^{81} and Gly^{85}. Interestingly, residues 85–90 adopt a different fold in each structure with the divergence beginning at residue 90 (reverse direction) (Fig. 1*B*). In the wild-type structure this loop remains close to the protein domain, whereas in PBP 5′ these residues point out toward solvent.

190–193 Loop—The only other region that is altered significantly between the two structures is the connecting loop between β7 and β8, comprising residues 190–193 (Fig. 1*B*). In the wild-type structure, this loop is displaced slightly away from the active site because of the presence of Met^{89}, which is central to the hydrophobic core in this region (see below). In the PBP 5′ structure, the absence of this residue has enabled Phe^{190} to move in and fill the void in the hydrophobic core.

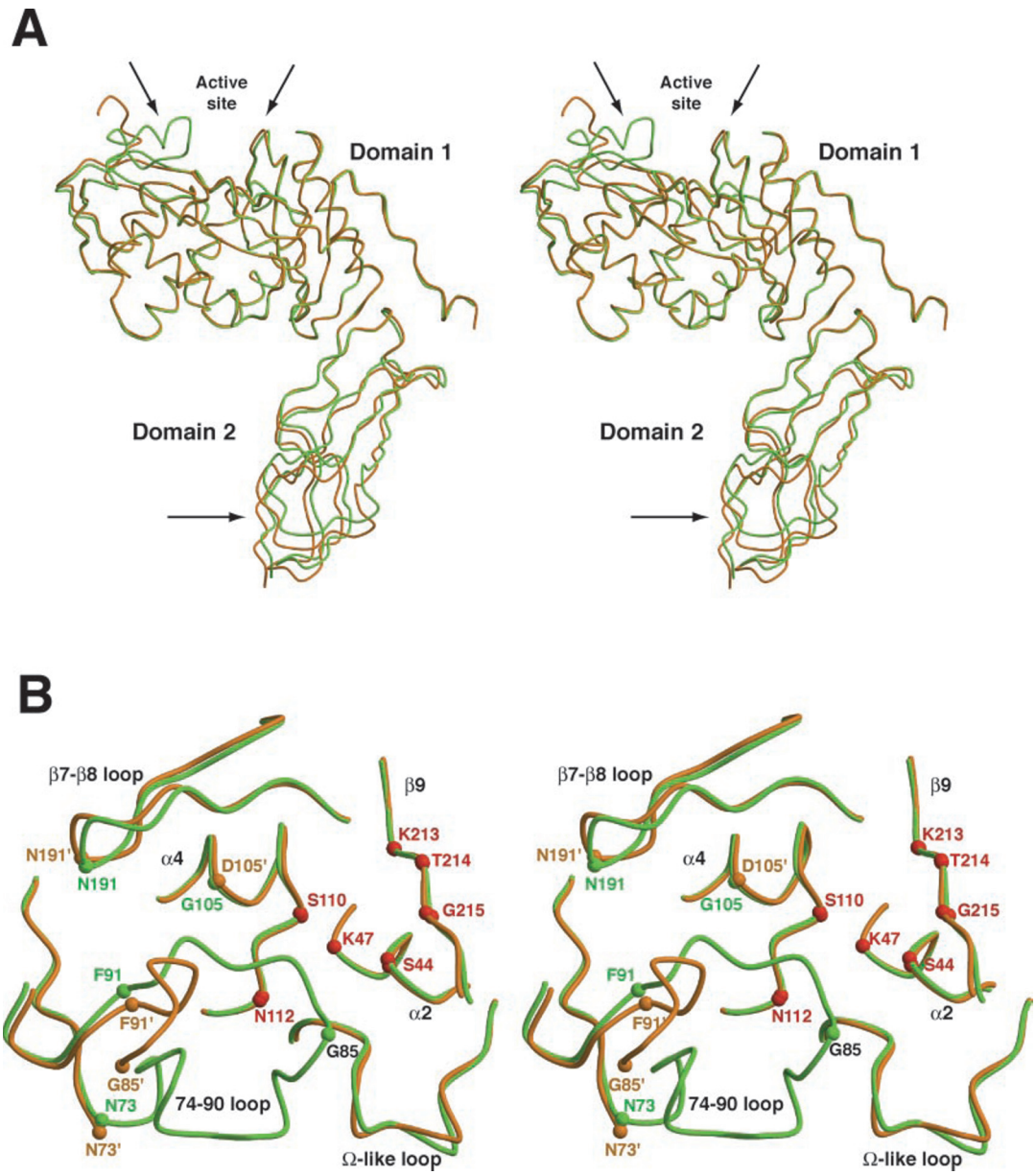

FIG. 1. **Comparison of the structures of wild-type PBP 5 and PBP 5-G105D mutant (PBP 5′).** *A*, stereo representation of the superimposition of the overall folds of the wild-type (*green*) and PBP 5′ mutant (*orange*) structures. The *arrows* denote the major regions of structural difference in the two proteins, located around the active site at the *top* and the *base* of the molecule in domain 2. *B*, stereo representation showing structural differences in the active site region. The secondary structure is labeled according to Davies *et al.* (20). The starting and ending points of the disordered region in PBP 5′ are denoted by the *small spheres* at the Cα atoms of residues 73 and 91, and are colored *orange* in PBP 5′, and *green* in wild-type. To emphasize the disparity between the two structures, the position of Gly^{85} is also shown in the wild-type structure (*green sphere*), which is located far from its counterpart in PBP 5′. For reference, Cα atoms of important active site residues are shown as *small red spheres*. This figure was prepared using MOLSCRIPT (36) and RASTER3D (37).

Effect of the G105D Mutation—Given that glycine residues tend to act as helix breakers, it might have been expected that the α4 helix containing the mutation would terminate earlier in wild-type PBP 5 than in the mutant PBP 5′ structure, thereby affecting the conformation of the S*X*N active site motif that directly follows the α4 helix. Surprisingly, little or no structural difference in this helix or its residue side chains is seen between the two structures (Fig. 2). In PBP 5′ only the side chain of Gln^{109} has moved slightly to avoid a clash with Asp^{105}, which lies directly below this residue on the helix. In the wild-type structure, the side chain of Gln^{109} is within hydrogen bonding distance of the carbonyl group of Leu^{88}, a contact that is absent in PBP 5′. Instead, the primary effect of the G105D mutation in PBP 5′ is to disrupt a hydrophobic core region. In the wild-type structure, this core is formed by the hydrophobic faces of α4, α5, β7, β8, and the 74–90 loop (Fig. 3). At the heart of the hydrophobic core is Met^{89}, with additional contributions of Phe^{188}, Phe^{190}, Leu^{91}, Leu^{102}, and Ala^{114}. In the PBP 5′ structure, a glycine to aspartic acid mutation at position 105 disrupts this region by projecting directly into the space occupied by Met^{89}. As a result, Met^{89} is displaced along with Phe^{90} and residues 85–88. The space vacated by Met^{89} is partially occupied by Phe^{190}, hence the movement of residues 190–193.

A buried aspartate (Asp^{113}) is also present within the hydrophobic core and each of its γ oxygen is within hydrogen bonding distance of three amide nitrogens (Fig. 4). $O^{\delta 1}$ of Asp^{113} contacts the amides of residues 89–91, whereas $O^{\delta 2}$ contacts the amides of 89, 113, and 114. The rarity of buried aspartates together with its role in stabilizing the structure of the 74–90 region suggests that the conformation of this loop is critical for

function. As discussed below, the change in conformation of residues 85 to 90 and the disordering of residues 74–84 is likely responsible for the altered kinetic properties of PBP 5′.

Active Site Comparison—A side-by-side comparison of the two active sites is shown in Fig. 5. The key residues are as follows: Ser^{44} and Lys^{47} of the Ser-*X*-*X*-Lys tetrad are located on one face of the α2 helix, Ser^{110} and Asn^{112} of the Ser-*X*-Asn triad are present on the loop connecting helices α4 and α5, and Lys^{213}, one of three residues in the Lys-Thr(Ser)-Gly triad, extends into the cavity. One other residue of note is Arg^{198}, which is on the loop at the top of the cavity. It is immediately obvious that the principal change in the active site in the wild-type structure results from the ordering of the loop encompassing residues 74–90 (shown as a *red loop* in Fig. 5*A*).

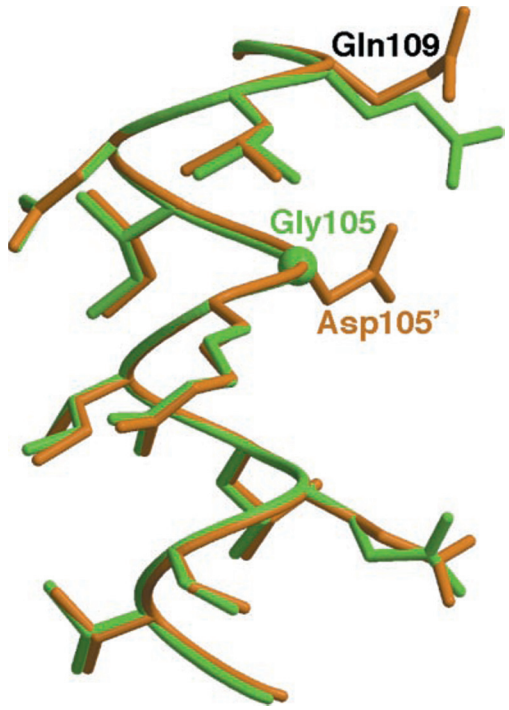

FIG. 2. **Superimposition of PBP 5 wild-type and PBP 5′ structures in the region of the mutation.** Both backbone and side chain residues show very little change in helix α4 containing the G105D mutation. The one exception is the side chain of Gln^{109}, which moves away in the mutant structure to accommodate the presence of the Asp mutation (see text for details). The color scheme is identical to Fig. 1. This figure was prepared using MOLSCRIPT (36) and RASTER3D (37).

This loop is oriented over the active site and interacts with the S*X*N motif via two serine residues, Ser^{86} and Ser^{87}, both of which are highly conserved in PBP 5-related CPases (20). Ser^{87} makes two potential hydrogen bonds, one between its side chain γ-oxygen and the carbonyl oxygen of Gln^{109} and the other from its carbonyl group to $N^{\delta 2}$ of Asn^{112} (Figs. 4 and 5). There is also a potential hydrogen bond between the γ-oxygen of Ser^{86} and $N^{\delta 2}$ of Asn^{112}. Thus Asn^{112} is contacted by Ser^{86}, Ser^{87}, and Lys^{47}. In PBP 5′ these serine-mediated interactions are absent because of the disordering of the 74–90 loop.

The relative positions of the residues comprising the conserved active site motifs of penicillin-interacting enzymes are essentially identical. The network of hydrogen bonding interactions observed in the PBP 5′ structure (20), those between Ser^{110} and Lys^{213}, and from Lys^{47} to Asn^{112} and the carbonyl of His^{151}, are all retained. One notable difference arises through a rotation of Ser^{44}, such that in the PBP 5′ structure this residue no longer forms a hydrogen bond with Lys^{47} (Figs. 5 and 6). The electron density for this residue in both structures, however, indicates some rotational freedom of the serine side chain. Arg^{198} is also oriented slightly different in the two structures because the presence of Ser^{87} on the 74–90 loop has pushed this residue upwards in the wild-type enzyme. The likely impact of these structural differences on catalytic function is discussed below.

Relatively few water molecules are observed in either active site and few are structurally conserved. The most significant water molecule is one within hydrogen bonding distance of Ser^{44} in both structures. In PBP 5′, a water molecule (Wat^{130}) bridges the γ oxygen of Ser^{44} and the carbonyl group of His^{216}. In the wild-type enzyme, a similar water molecule is present (called Wat^{89}) but because Ser^{44} is rotated slightly with respect to PBP 5′, the water is too distant to hydrogen bond with His^{216}.

Functional Analysis of PBP 5 Mutants and Variants Lacking Residues 72–90—As discussed above, the structure of wild-type PBP 5 reported here differs from PBP 5′ primarily by the ordering of the region encompassing residues 74–90. This result suggests that the functional phenotype of PBP 5′, *i.e.* a markedly impaired deacylation rate and lack of CPase activity, is due directly to the disruption of this region by the G105D mutation. To test this hypothesis and to determine the role of the 74–90 loop in the activity of PBP 5, we made constructs in which this loop was deleted. In the wild-type structure, the α carbons of residues 71 and 93 are separated by 4.7 Å. Because the residue following Pro^{93} is a glycine, we predicted that

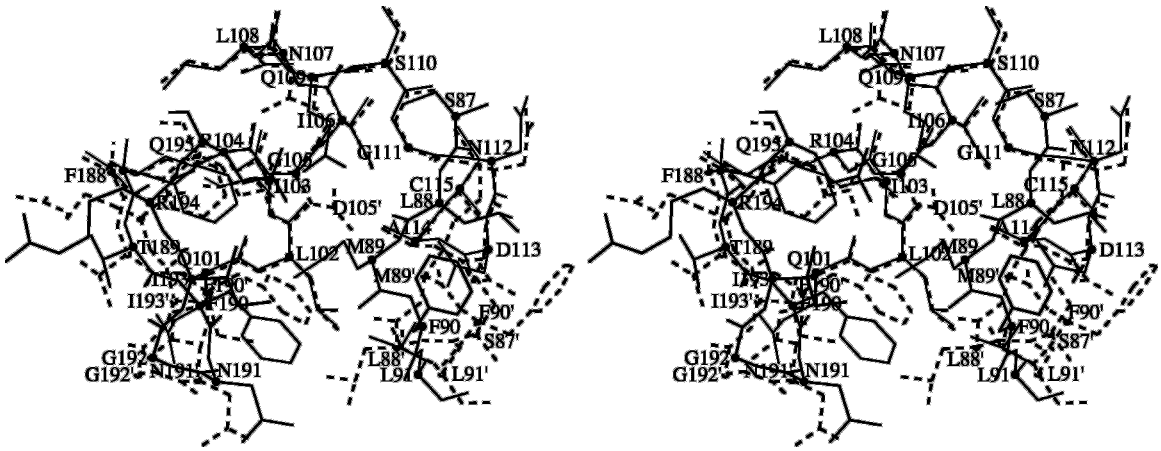

FIG. 3. **Stereo representation of the hydrophobic core region in wild-type PBP 5.** This region is formed in part by the 74–90 loop, which is altered in PBP 5′. In this superimposition the wild-type structure is shown as *solid bonds*, whereas the PBP 5′ structure is shown as *dashed lines*. The α carbon positions are shown as *dots* and are labeled. In areas where the structures diverge, the equivalent atoms in PBP 5′ are also labeled. This figure was prepared using MOLSCRIPT (36).

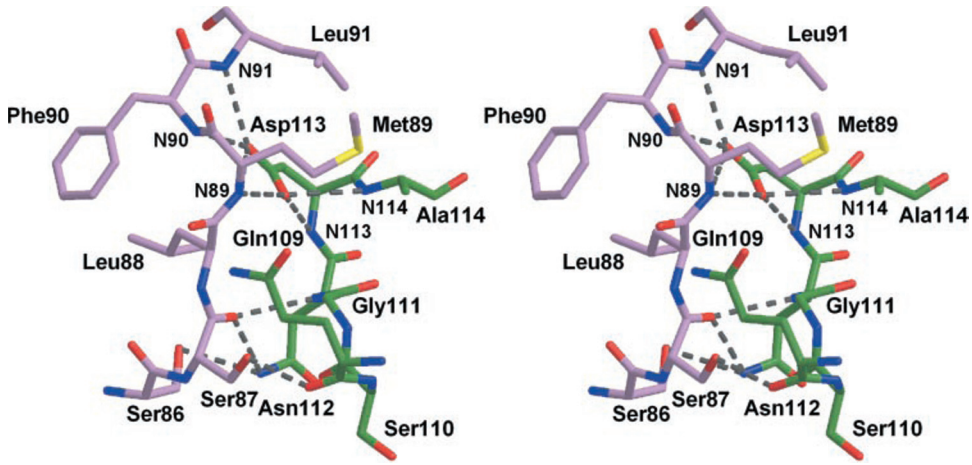

FIG. 4. **Stereo representation of the interactions made between the 74–90 loop (*colored purple*) and the SXN active site motif (*colored green*) in PBP 5.** In this view the active site is at the *bottom*. Three residues are particularly important in this interface: Asp^{113} makes several interactions with the backbone of residues 89–91, 113, and 114, and serines 86 and 87 interact directly with Ser^{110} and Asn^{112} of the SXN motif. Potential hydrogen bonds are shown as *dashed lines*. Oxygen and nitrogen atoms are shown as *red* and *blue bonds*, respectively. This figure was prepared using MOLSCRIPT (36) and RASTER3D (37).

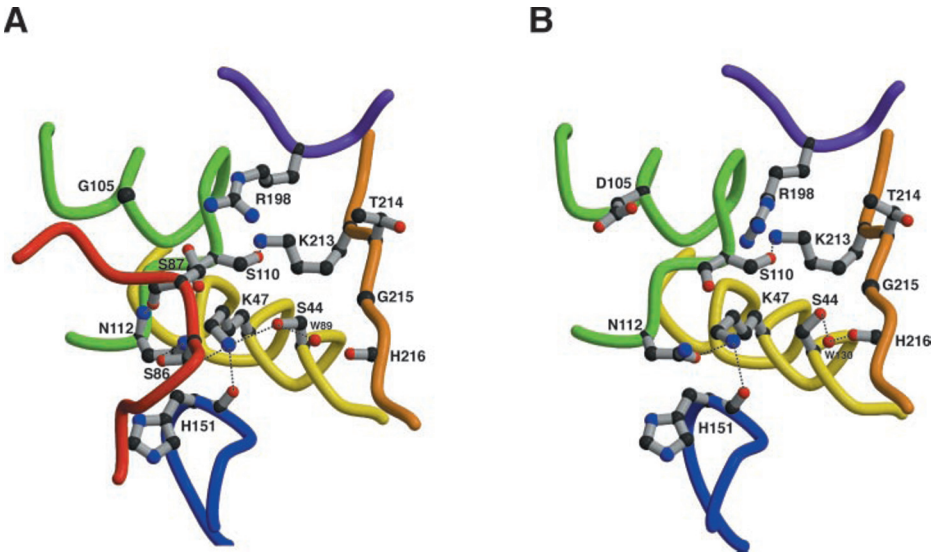

FIG. 5. **A side-by-side comparison of active site residues in (*A*) wild-type and (*B*) G105D mutant PBP 5.** The active site is formed by five structural elements. Three of these contain the well known sequence motifs typical of penicillin-interacting enzymes: the S*XXK* motif (*yellow*), the SXN motif (*green*), and the KTG motif (*orange*). Other motifs are specific to PBP 5 and close homologues: the Ω-like loop (*blue*), a loop containing Arg^{198} (*purple*) and the 74–90 region (*red*). Note the absence of the latter in PBP 5′. *Dashed lines* indicate potential hydrogen bonds. This figure was prepared using MOLSCRIPT (36) and RASTER3D (37).

fusing Ile^{71} to Pro^{93} would promote the formation of a β-turn with minimal disturbance to the overall structure of the protein.

PBP 5, PBP 5′, and both proteins missing residues 72–92 (termed PBP 5-LO and PBP 5′-LO, respectively) were expressed in *E. coli* and purified by ampicillin affinity chromatography. Like PBP 5 and PBP 5′, the loop-out constructs were soluble and bound stoichiometric amounts of [^{14}C]penicillin G (data not shown). Internal deletion of residues 72–92 had only a small effect on the specificity constant for penicillin G. Wild-type PBP 5 had a k_2/K' of 390 M^{-1} s^{-1} with [^{14}C]penicillin G, whereas PBP 5′, PBP 5-LO, and PBP 5′-LO had k_2/K' values ~4- to 6-fold lower (Table II). Moreover, the k_2/K' values for the two loop-out constructs were very similar to the k_2/K' constant for PBP 5′, and effects of the loop-out were not additive with the G105D mutation.

In contrast to the small effect on the acylation rate constants in the loop-out constructs, there was a much greater effect on the deacylation rates of the penicilloyl-PBP 5 complex. PBP 5 and PBP 5′ hydrolyzed bound [^{14}C]penicillin G with rate constants of 78×10^{-4} s^{-1} ($t_{1/2}$ = 14.4 min) and 3×10^{-5} s^{-1} ($t_{1/2}$ = 380 min), respectively, which were very similar to the constants reported previously (16, 31) (Table II). Consistent with our hypothesis, PBP 5-LO had a deacylation rate constant of 3.7×10^{-5} s^{-1} ($t_{1/2}$ = 315 min), very similar to the k_3 rate constant of PBP 5′. Thus, deletion of residues 72–92 in PBP 5 had essentially the same affect on deacylation as mutation of Gly^{105} to Asp. When residues 72–92 were deleted in PBP 5′, the k_3 constant decreased another 3-fold to 1.1×10^{-5} s^{-1} ($t_{1/2}$ = 1050 min).

Another characteristic of PBP 5′ is its lack of CPase activity. If the major effect of the G105D mutation is the disruption of the region encompassing residues 74–90, we would expect that the loop-out constructs would also lack CPase activity. Indeed, both PBP 5-LO and PBP 5′-LO lack any detectable CPase activity with *N*,*N*′-diacetyl-L-Lys-D-Ala-D-Ala, even at peptide concentrations as high as 10 mM and enzyme concentrations as high as 8 μM. The loss of CPase activity in both PBP 5′ and PBP 5-LO could result from one of two scenarios: 1) the peptide forms an acyl-enzyme complex but is unable to undergo deacylation (*i.e.* no turnover), or 2) the peptide is incapable of forming an acyl-enzyme complex, either because of a lack of substrate binding or acylation. To distinguish between these two possibilities, we incubated PBP 5 and PBP 5-LO with or without 20 mM peptide substrate at pH 8.5 for 20 min prior to assessing their acylation rate with [^{14}C]penicillin G. There was no difference in the k_2/K' constants between buffer and peptide preincubation conditions (data not shown), precluding the possibility that the peptide

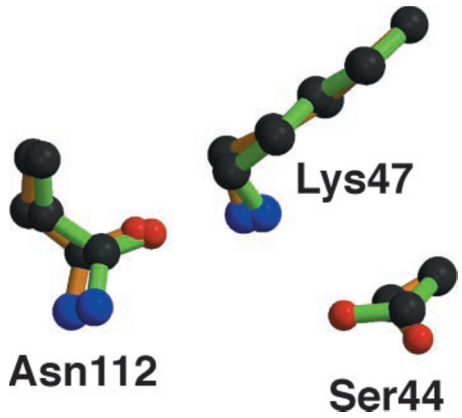

FIG. 6. **Superimposition of three active site residues from wild-type and G105D mutant structures of PBP 5.** Atoms are colored by type in which oxygens are *red*, nitrogens are *blue*, and carbons are *dark gray*. Bonds are colored *green* for wild-type and *orange* for G105D mutant. Note the minimal difference in the conformation of Asn^{113}, even though in wild-type PBP 5 this residue interacts with serines 86 and 87 (not shown but to the *left*). This figure was prepared using MOLSCRIPT (36) and RASTER3D (37).

TABLE II
Kinetic constants for the interaction of PBP 5 variants with [^{14}C]penicillin G and peptide substrate

k_2/K' and k_3 values were determined as described under "Materials and Methods" and are the average of three to seven independent experiments. The k_{cat}/k_m values were determined with the synthetic peptide substrate, *N,N'*-diacetyl-L-Lys-D-Ala-D-Ala.

Protein	k_2/K'	$t_{1/2}$	k_3	k_{cat}/K_m
	$M^{-1}\ s^{-1}$	*min*	$s^{-1} \times 10^{-5}$	$M^{-1}\ s^{-1}$
PBP 5	390 ± 80	14.4 ± 0.8	78 ± 4	32 ± 5
PBP 5′(G105D)	80 ± 14	380 ± 14	3.0 ± 0.1	ND[a]
PBP 5-LO	73 ± 6	315 ± 14	3.7 ± 0.2	ND
PBP 5′-LO	120 ± 10	1050 ± 44	1.1 ± 0.1	ND
PBP 5-S86A	270 ± 20	38 ± 7	32 ± 2	3.9 ± 0.8
PBP 5-S87A	310 ± 30	33 ± 2	35 ± 2	2.0 ± 0.5
PBP 5-S86A,S87A	305 ± 12	20 ± 0.3	58 ± 1	2.6 ± 0.5

[a] ND, no activity detected.

substrate forms a stable acyl-enzyme complex.

We also investigated the role of the two serine residues (Ser^{86} and Ser^{87}) in the 74–90 loop, which are conserved in PBP 5-related CPases (20). As discussed above, these residues sit atop the S*X*N active site motif and contact both the main chain and side chain amides of Asn^{112} and the main chain carbonyl of Gln^{109} (Fig. 4). Ser^{86} and Ser^{87} were mutated to alanine, and the enzymatic and kinetic activities of the resulting proteins were determined. Mutation of these serine residues either individually or together had little effect on the interaction of the protein with [^{14}C]penicillin G (Table II). The acylation rate constants of the mutants were nearly identical to wild-type PBP 5, suggesting these residues serve no role in binding or acylation of β-lactam antibiotics. The mutants showed only a slight decrease in k_3 with [^{14}C]penicillin G, between 1.4- and 2.6-fold lower than wild-type (Table II). In contrast, all the serine mutants showed a much greater decrease (between 8- and 16-fold) in the k_{cat}/K_m constants for CPase activity measured with peptide substrate. These data suggest that these two serine residues are important for CPase activity of PBP 5.

DISCUSSION

Our structural studies of PBP 5 began with PBP 5-G105D (called PBP 5′), a deacylation-defective mutant of PBP 5 (20). This structure revealed that PBP 5 has two domains: a penicillin-binding domain showing high structural similarity to other PBPs and class A β-lactamases, and a second domain of unknown function. In the absence of structural information for the wild-type enzyme, however, the mutant structure provided little insight into how the G105D mutation leads to a catalytic deficiency in deacylation. In this study, we present the structure of wild-type PBP 5 determined to 1.85-Å resolution and compare it with the previous structure of PBP 5′ now refined to 1.9-Å resolution. The striking difference between the two structures is the order/disorder in residues 74–90, suggesting that this region is critical for catalytic function. This hypothesis is supported by the apparent precision in its structure and by its close proximity to the active site. Most striking is the presence of a buried aspartate (Asp^{113}) that orients the loop via interactions with the amide nitrogens of residues 89–91, an interaction that is lost in PBP 5′ (see Fig. 4). Buried aspartates are rare in proteins and their presence usually signifies a region important for function. Another unusual feature is the zig zag structure that immediately precedes Ser^{86} and Ser^{87}.

Disordering of the loop encompassing residues 74–90 in PBP 5′ could arise in two ways: 1) through differences in crystal packing between the two crystal forms or 2) as a direct effect of the G105D mutation. In essence, this is a chicken and egg problem. Did the crystal packing in the $P3_2$ form afford the loop greater flexibility, leading to its disorder, or did the mutation disrupt the loop and thereby prevent crystallization of PBP 5′ in the C2 space group? Several lines of evidence suggest the latter explanation is most likely. First, the wild-type protein does not crystallize under the same conditions obtained for PBP 5′, which suggests that the protein structure itself determines the crystal form and not vice versa. Second, examination of the wild-type structure shows an obvious mechanism for how the mutation site disrupts the 74–90 loop. In the mutant enzyme Asp^{105} displaces Met^{89} from a hydrophobic core and in doing so alters the loop structure and hence the crystallization behavior of the protein. Finally, removal of the loop by deleting the codons encoding residues 72–92 results in a protein with a nearly identical functional phenotype as PBP 5-G105D, suggesting that the disordering of the loop leads directly to the decrease in deacylation of [^{14}C]penicillin G and abrogation of CPase activity.

Comparison of the PBP 5 and PBP 5-G105D structures does not reveal an obvious mechanism for the loss of CPase activity in PBP 5′, especially because the 74–90 loop appears too far removed from the active site to participate directly in catalysis. One explanation is that PBP 5′ retains the ability to bind and react with peptide and that the loss of CPase activity is because of the marked decrease in the rate of deacylation, resulting in the accumulation of covalently bound peptide. However, this is unlikely because preincubation of PBP 5-LO with peptide had no effect on the rate of acylation with [^{14}C]penicillin G. A more likely explanation is that this region is important for peptide binding (and/or acylation) but to test this will require a complex of PBP 5 with peptide substrate.

One contributing factor to the loss of peptide binding in PBP 5′ and PBP 5-LO may be the movement of Arg^{198}, which sits at the top of the active site (Fig. 5). In PBP 5′, Arg^{198} forms a hydrogen bond with the carbonyl of Gln^{109}, whereas in the wild-type enzyme it is hydrogen-bonded to Ser^{87}. The recent structure of the *Streptomyces* R61 D,D-peptidase in complex with its peptide substrate revealed a strong interaction between Arg^{285}, the equivalent of Arg^{198} in the D,D-peptidase, and the C-terminal carboxylate of the peptide substrate (32). Thus, the altered position of Arg^{198} in PBP 5′ (and presumably PBP 5-LO) may hamper its ability to interact with the C terminus of the peptide substrate in PBP 5, leading to a marked decrease in substrate binding and CPase activity.

Our results shed new light on the mechanism of deacylation in PBP 5. The wild-type and G105D mutant PBP 5 structures, together with kinetic analysis of the loop-out constructs, suggest that disordering of the 74–90 loop is the primary reason for the defect in the rate of hydrolysis of the acyl-enzyme complex in PBP 5′. Furthermore, the precise interaction of this region with the active site via contacts from serines 86 and 87 to the S*X*N motif suggests that this motif has a major role in deacylation of the acyl-enzyme complex. How it does so is unclear. Its absence or presence makes almost no difference to the conformation of the S*X*N motif (Fig. 6), suggesting a subtle mechanism for the defect in deacylation in PBP 5′. Moreover, mutation of these residues to alanine had no effect on acylation with β-lactam antibiotics and only minor effects on deacylation. In contrast, we observed a ~10-fold decrease in k_{cat}/K_m for hydrolysis of peptide substrate, clearly implicating these residues in CPase activity. Interestingly, the functional phenotype resulting from mutation of these two serine residues in PBP 5 was much less severe than that obtained by deleting the 74–90 loop, which resulted in a 30-fold decrease in deacylation activity and the total absence of CPase activity. At first glance this appears to suggest a role for this loop beyond that of orienting these two serine residues. However, because several of the hydrogen bonds from these two serines to residues in the S*X*N motif emanate from the peptide backbone and would be retained in the mutants, the severity of the functional phenotype in PBP 5′ and PBP 5-LO may simply be because of the absence of these backbone-mediated interactions.

How then does the S*X*N motif function in deacylation? The two obvious candidates for a functional role are Asn^{112} and Ser^{110}: Asn^{112} is contacted directly by both Ser^{86} and Ser^{87}, whereas Ser^{110} is contacted indirectly via interactions from Ser^{87} to Gln^{109} and Gly^{111} (see Fig. 4). In class C β-lactamases and the D,D-peptidase from *Streptomyces* R61, the equivalent residue of Ser^{110} is a tyrosine and the phenoxide anion of this residue has been proposed to act as a general base in deacylation (33–35). For Ser^{110} in PBP 5 to act in an analogous manner, however, seems unlikely because the pK_a of the serine hydroxyl is too high for this residue to form an anion. The same argument applies to Asn^{112} and so it is doubtful that either of these residues act directly in deacylation. Instead we have assigned Lys^{47} as the general base to polarize the hydrolytic water molecule, which is located next to Ser^{44} (11, 20). A more likely role for either Ser^{110} or Asn^{112} would be to help orient the hydrolytic water molecule near Lys^{47}. Asn^{112} is suitably positioned immediately adjacent to Lys^{47} (Fig. 6) and for Ser^{110}, its side chain could rotate away from Lys^{213} and toward Lys^{47} (see Fig. 5*A*). Regardless of which residue is involved, it is clear that the absence of the 74–90 loop in PBP 5′ hinders deacylation. To investigate the role of the 74–90 loop in deacylation further will require structures of both PBP 5 and PBP 5′ covalently bound to penicillin G in which the hydrolytic water is apparent. These studies are underway.

REFERENCES

1. Ghuysen, J. M. (1991) *Annu. Rev. Microbiol.* **45,** 37–67
2. Tipper, D. J., and Strominger, J. L. (1965) *Proc. Natl. Acad. Sci. U. S. A.* **54,** 1133–1141
3. Wise, E. M., Jr., and Park, J. T. (1965) *Proc. Natl. Acad. Sci. U. S. A.* **54,** 75–81
4. Waxman, D., and Strominger, J. L. (1980) *J. Biol. Chem.* **255,** 3964–3976
5. Joris, B., Ghuysen, J.-M., Dive, G., Renard, A., Dideberg, O., Charlier, P., Frere, J.-M., Kelly, J. A., Boyington, J. C., Moews, P. C., and Knox, J. R. (1988) *Biochem. J.* **250,** 313–324
6. Adachi, H., Ohta, T., and Matsuzawa, H. (1991) *J. Biol. Chem.* **266,** 3186–3191
7. Guillaume, G., Vanhove, M., Lamotte-Brasseur, J., Ledent, P., Jamin, M., Joris, B., and Frere, J. M. (1997) *J. Biol. Chem.* **272,** 5438–5444
8. Lewis, E. R., Winterberg, K. M., and Fink, A. L. (1997) *Proc. Natl. Acad. Sci. U. S. A.* **94,** 443–447
9. Gutheil, W. G. (1998) *Anal. Biochem.* **259,** 62–67
10. Gutheil, W. G., Stefanova, M. E., and Nicholas, R. A. (2000) *Anal. Biochem.* **287,** 196–202
11. Stefanova, M. E., Davies, C., Nicholas, R. A., and Gutheil, W. G. (2002) *Biochim. Biophys. Acta* **1597,** 292–300
12. Matsuhashi, M., Tamaki, S., Curtis, S. J., and Strominger, J. L. (1979) *J. Bacteriol.* **137,** 644–647
13. Nelson, D. E., and Young, K. D. (2000) *J. Bacteriol.* **182,** 1714–1721
14. Begg, K. J., Dewar, S. J., and Donachie, W. D. (1995) *J. Bacteriol.* **177,** 6211–6222
15. Amanuma, H., and Strominger, J. L. (1980) *J. Biol. Chem.* **255,** 11173–11180
16. Nicholas, R. A., and Strominger, J. L. (1988) *J. Biol. Chem.* **263,** 2034–2040
17. Matsuhashi, M., Maruyama, I. N., Takagaki, Y., Tamaki, S., Nishimura, Y., and Hirota, Y. (1978) *Proc. Natl. Acad. Sci. U. S. A.* **75,** 2631–2635
18. Broome-Smith, J. K., and Spratt, B. G. (1984) *FEBS Lett.* **165,** 185–189
19. Amanuma, H., and Strominger, J. L. (1984) *J. Biol. Chem.* **259,** 1294–1298
20. Davies, C., White, S. W., and Nicholas, R. A. (2001) *J. Biol. Chem.* **276,** 616–623
21. Pflugrath, J. W. (1999) *Acta Crystallogr. Sect. D Biol. Crystallogr.* **55,** 1718–1725
22. Navaza, J. (1994) *Acta Crystallogr. Sect. A* **50,** 157–163
23. Brünger, A. T. (1992) *X-PLOR, Version 3.1, A System for X-ray Crystallography and NMR*, Yale University, New Haven, CT
24. Murshudov, G. N., Vagin, A. A., and Dodson, E. J. (1997) *Acta Crystallogr. Sect. D Biol. Crystallogr.* **53,** 240–255
25. Jones, T. A., Zhou, J. Y., Cowan, S. W., and Kjeldgaard, M. (1991) *Acta Crystallogr. Sect. A* **47**, 110–119
26. Laskowski, R. A., MacArthur, M. W., Moss, D. S., and Thorton, J. M. (1993) *J. Appl. Crystallogr.* **26,** 283–291
27. Collaborative Computation Project, N. (1994) *Acta Crystallogr. Sect. D Biol. Crystallogr.* **50,** 760–763
28. Ho, S. N., Hunt, H. D., Horton, R. M., Pullen, J. K., and Pease, L. R. (1989) *Gene* (*Amst.*) **77,** 51–59
29. Tabor, S., and Richardson, C. C. (1985) *Proc. Natl. Acad. Sci. U. S. A.* **82,** 1074–1078
30. Frere, J. M., Nguyen-Disteche, M., Coyette, J., and Joris, B. (1992) in *The Chemistry of β-Lactams*, pp. 148–196, Chapman and Hall, Glasgow
31. Malhotra, K. T., and Nicholas, R. A. (1992) *J. Biol. Chem.* **267,** 11386–11391
32. McDonough, M. A., Anderson, J. W., Silvaggi, N. R., Pratt, R. F., Knox, J. R., and Kelly, J. A. (2002) *J. Mol. Biol.* **322,** 111–122
33. Oefner, C., D'Arcy, A., Daly, J. J., Gubernator, K., Charnas, R. L., Heinze, I., Hubschwerlen, C., and Winkler, F. K. (1990) *Nature* **343,** 284–288
34. Dubus, A., Ledent, P., Lamotte-Brasseur, J., and Frere, J. M. (1996) *Proteins* **25,** 473–485
35. Silvaggi, N. R., Anderson, J. W., Brinsmade, S. R., Pratt, R. F., and Kelly, J. A. (2003) *Biochemistry* **42,** 1199–1208
36. Kraulis, P. J. (1991) *J. Appl. Crystallogr.* **24,** 946–950
37. Merritt, E. A., and Murphy, M. E. P. (1994) *Acta Crystallogr. Sect. D Biol. Crystallogr.* **50**, 869–873